Food Chemistry 256 (2018) 62–70

Contents lists available at ScienceDirect

Food Chemistry

journal homepage: www.elsevier.com/locate/foodchem

Physical, thermal and thermodynamical study of high oleic palm oil nanoemulsions

Leidy Ricaurte, Maria Hernández-Carrión, Miguel Moyano-Molano, Angélica Clavijo-Romero, María Ximena Quintanilla-Carvajal*

Facultad de Ingeniería, Universidad de La Sabana, km 7 vía autopista Norte, Bogotá, Colombia

ARTICLE INFO

Keywords:
Nanoemulsions
Thermodynamic
Stability
Ostwald ripening
High oleic palm oil

ABSTRACT

Nanoemulsions are useful for encapsulating nutritionally compounds of the high oleic palm oil (HOPO) including β-carotene and tocopherols. However, some nanoemulsions can be thermodynamically unstable. For this reason, it is important to understand the thermal and thermodynamic stability of nanoemulsions and to investigate both the parameters that cause, and the mechanisms associated with, the destabilization. In this sense, the DSC, TGA and destabilization analysis were used. In this work, the average droplet size (ADS) and zeta potential (ζ) had a significant influence over HOPO nanoemulsions stability. The range of ADS and ζ were between 162 and 839 nm and −9 to −40 mV, respectively. Furthermore, the HOPO nanoemulsions were establish until temperatures of 80 °C, showing lower loss of weight when the ADS was higher. Additionally, the destabilization of nanoemulsions occurred by the Ostwald ripening mechanism. The Ostwald ripening rate was provided as stability parameter which increased to nanoemulsions with ADS higher between 5×10^{-23} and 8×10^{-23} m^3/s.

1. Introduction

Emulsions are colloidal systems in which the oily phase is dispersed in a stable aqueous form. However, such systems are thermodynamically unstable, which directly affects their useful lifetime. Thermodynamic instability is a constraint that needs to be improved in emulsions, as it is largely determined by the type of emulsifier employed. Therefore, the selection of the best combination of emulsifier concentrations is necessary to design stable emulsions.

In this work, different emulsions were obtained using two food-grade emulsifying agents: gelatin and lecithin. Gelatin consists of proteins that have excellent emulsifying characteristics due to their amphiphilic nature, that is, the presence of both hydrophilic and hydrophobic amino acids, which are oriented towards the surface of the oil-water interface for stabilization (Primozic, Duchek, Nickerson, & Ghosh, 2017). In contrast, lecithin is a mixture of phospholipids and neutral lipids, which have two ends, one positively charged and the other containing several unsaturated chains (Nirmala et al., 2011). Moreover, as a stabilizing material and possible wall material, whey was used because it showed a high oil protection capacity (Ricaurte, Perea-Flores, Martinez, & Quintanilla-Carvajal, 2016).

The mechanisms under which emulsions can be destabilized are cremation, flocculation, sedimentation and Ostwald ripening. The latter is the most common mechanism for the destabilization of nanoemulsions (Wooster, Golding, & Sanguansri, 2008), as it describes the growth of small droplets into larger ones by the molecular diffusion of the oil through the continuous phase (Wooster et al., 2008). In addition, this process can be studied by measuring the droplet size, electrophoretic mobility and turbidimetry, among other properties.

Since emulsions are systems that tend to be used in encapsulation processes, which involve the protection of an oil, for this work, high oleic palm oil (HOPO) was chosen because of the benefits it possesses. It contains high concentrations of β-carotene and vitamin E (between 500–1080 ppm and 110–600 ppm, respectively (Cuellar, 2016)), which may contribute to the reduction of deficiencies in these vitamins in developing countries such as Colombia. In addition, it is relevant to mention that the composition of crude HOPO is different from that of African palm oil. The saturated and unsaturated fatty acid compositions of HOPO (hybrid between *Elaeis guineensis* and *Oleifera*) are 27–39% and 58–72% (Hacienda La Cabaña, 2012), respectively, while African palm oil (*Elaeis guineensis* Jacq.) contains approximately 50% saturated and 50% unsaturated fatty acids (Obahiagbon, 2012). It is because of this high content of oleic acid that this oil is considered as healthy as olive oil (Segall & Artz, 2005).

Therefore, the objective of this work was to establish the physical characteristics as well as thermal and thermodynamic stabilities of

* Corresponding author.
E-mail address: maria.quintanilla1@unisabana.edu.co (M.X. Quintanilla-Carvajal).

https://doi.org/10.1016/j.foodchem.2018.02.102
Received 16 November 2017; Received in revised form 16 February 2018; Accepted 19 February 2018
Available online 21 February 2018

HOPO nanoemulsions obtained by microfluidization as encapsulation systems.

2. Material and methods

2.1. Materials

The materials used to produce HOPO nanoemulsions were high oleic palm oil (Hacienda la Cabaña, Colombia) donated by the Centro de Investigación del Cultivo de Palma (Center for Research on Palm Cultivation; CENIPALMA), whey and gelatin obtained in a local supermarket, soy lecithin (PubChem CID: 57369748) (Bell Chem, Colombia) and distilled water.

2.2. Preparation of coarse emulsions

Coarse emulsions were homogenized with a mixer obtained from a local supermarket (Oster, Colombia). First, sweet whey was dissolved in water, and heated using a microfluidizer LM10 (Microfluidics International Corporation, MA, USA) at 20,000 psi for four cycles. The equipment was used to ensure the dissolution of the gelatin. In parallel, HOPO and a constant lecithin concentration (10% w/w with respect to HOPO) were manually mixed and added to the water-gelatin-whey mixture. The total mixing time with all the ingredients was approximately 2 min.

2.3. Preparation of nanoemulsions

The HOPO nanoemulsions were obtained following previously published methodology (Ricaurte et al., 2016). Briefly, the nanoemulsions were homogenized in an LM10 microfluidizer (Microfluidics, England) following a response optimization design obtained with Design Expert Version 8.1.0 software (Stat-Ease Inc., MN, USA). The factors that were varied were variables related to the nanoemulsion formulation (whey, HOPO and gelatin concentrations) and variables related to the microfluidizer operating conditions (pressure and cycles). Table 1 shows the conditions obtained from the response optimization design for the preparation of nanoemulsions.

2.4. Nanoemulsion characterization

HOPO nanoemulsions were characterized with respect to their physical characteristics such as the average droplet size (ADS), polydispersity index (PdI), zeta potential (ζ), surface tension, conductivity and flow behavior. Additionally, the thermal and thermodynamic stabilities of the nanoemulsions were studied as described below.

2.4.1. Droplet size, polydispersion index and zeta potential

The average droplet size (ADS), polydispersion index (PdI) and zeta potential (ζ) were determined using dynamic light scattering equipment (DLS) with a Zetasizer NanoZS laser diffractometer (Malvern Instruments, England) using a water dilution of 1:1000 (v/v). The measurements were performed in duplicate with a dispersion angle of 173°.

2.4.2. Surface tension

The surface tension (ST) of the nanoemulsions was measured following the methodology of Teixeira et al. (2017) with some modifications. The Sigma 700 tensiometer (Attension, Finland) equipped with Wilhelmy plate at room temperature (19 °C) with 20 mL of sample was placed in a standard glass vessel to perform the measurement in duplicate.

2.4.3. Conductivity

The conductivities of the nanoemulsions were determined using a 2306.0 (DELTA OHM) conductivity meter. Measurements were performed in duplicate and reported as the average.

2.4.4. Flow curve

The flow behaviors of the nanoemulsions were studied on an MCR 502 rheometer (Anton Paar, Germany) with a 49.97 mm parallel plate geometry (PP50) using a 0.5 mm gap over a shear rate interval of 1–100 s^{-1}. Approximately 1.2 mL of the sample was carefully placed on the lower plate. Nanoemulsions exhibited Newtonian behavior (linear shear stress adjustment as a function of the shear rate was fitted with an average R^2 of 0.99 (data not shown)). The viscosity was reported at a shear rate of 75 s^{-1}.

2.5. Thermal and thermodynamic stabilities of nanoemulsions

The thermal and thermodynamic stabilities were evaluated for two optimized HOPO emulsions from the minimum and maximum droplet sizes (min-opt and max-opt respectively) with high values of stability (minimum ζ value), whose preparation conditions are shown in Table 3 (in the Section 2.6 the statistical procedure is explained).

2.5.1. Differential scanning calorimetry and thermal gravimetric analysis

The thermal stabilities of optimized HOPO emulsions (min-opt and max-opt) were determined using differential scanning calorimetry (DSC, DSC 3+, Mettler Toledo, USA). The sample (approximate weight 12–13 mg) was placed in hermetically sealed aluminum foil for analysis. Heat treatment applied was from −15 °C to 70 °C with a ramp of 1 °C/min. This maximum temperature of 70 °C was established because the applications of the HOPO nanoemulsions are directed toward the food industry, where that is the maximum average temperature applied in different processes.

The change in mass as a function of temperature was determined with thermogravimetric analysis (TGA/DSC1 Stare System, Metter Toledo, Germany) using the associated software STARe version 11.0.

2.5.2. Destabilization mechanism by Ostwald ripening

To establish the mechanism of destabilization of HOPO emulsions (min-opt and max-opt), the thermodynamic stability was associated with the change in the average droplet size as a function of time, following the methodology of Noor El-Din, El-Hamouly, Mohamed, Mishrif, and Ragab (2013). The samples were centrifuged at 500 rpm at 20 °C (Mettler Toledo, USA) for 5, 10, 20, 30, 40, 50 and 60 min. Subsequently, the average droplet size of the surface layer was determined using the methodology of Section 2.4.1. The Ostwald ripening mechanism is described by the following Eq. (1):

$$\omega = \frac{dr^3}{dt} = \frac{8}{9}\left[\frac{C_\infty \gamma V_m}{dRT}\right] \quad (1)$$

where r is the average radius of the droplet, t is the storage time. The Ostwald ripening rate can be calculated from the slope of each straight line.

2.6. Statistical analysis

Statistical analysis was performed based on the response surface methodology for optimization experimental design using the software Design Expert Version 8.1.0 (Stat-Ease Inc., MN, USA).

Linear, quadratic and logarithmic models were used to express the response variables as a function of the independent factors, where A, B, C, D and E are the coded values of whey concentration, oil concentration, gelatin concentration, pressure and number of cycles, respectively. A statistical significance test was used in the total error criteria with a confidence level of 95%. Significant terms in the model were found by analysis of variance (ANOVA). The model fit was evaluated by the R^2 value. The graphical and numerical optimization technique of the Design Expert software was used for the optimization of the response following the criterion of desirability (Jeong & Kim, 2009).

Table 1
Response optimization surface experimental design methodology for preparation of nanoemulsions and adjusted variables to the model: ADS, PdI, ζ, conductivity, ST and viscosity.

Run	Whey concentration [A] (%w/w)	HOPO concentration [B] (%w/w)	Gelatin concentration [C] (%w/w)	Pressure [D] (psi)	Cycles [E]	ADS (nm)	PdI	ζ (mV)	Conductivity (mS)	ST (mN/m)	Viscosity (mPa·s)
1	25.00	10.00	0.00	8000	1	759.00	0.65	−31.67	10.72	29.41	9.24
2	0.00	10.00	0.00	8000	3	226.30	0.21	−45.00	0.21	23.92	1.32
3	13.38	0.00	0.05	12,860	1	162.60	0.18	−26.50	8.33	44.04	1.42
4	0.25	5.05	0.99	14,600	4	367.85	0.37	−20.85	0.55	31.29	2.20
5	12.88	4.25	1.00	8000	2	607.35	0.60	−23.85	8.48	31.05	4.12
6	14.25	0.00	0.50	20,000	4	162.95	0.28	−21.75	11.68	48.16	1.89
7	25.00	0.00	1.00	8000	4	165.60	0.16	−21.50	16.11	47.78	9.34
8	1.13	0.00	0.63	15,680	2	240.30	0.33	−9.52	1.30	48.85	1.19
9	0.00	4.80	0.60	8000	1	305.97	0.20	−24.40	0.17	38.30	1.71
10	25.00	0.00	0.05	8000	2	161.00	0.20	−25.20	13.29	51.42	6.40
11	0.00	10.00	0.00	20,000	4	368.40	0.39	−37.30	0.28	29.44	1.65
12	0.00	10.00	1.00	20,000	2	256.05	0.31	−28.95	0.23	21.96	1.45
13	0.00	0.00	1.00	8000	3	352.45	0.42	−7.19	0.11	44.14	1.30
14	20.00	1.73	1.00	17,600	3	257.80	0.26	−23.40	11.07	41.28	4.31
15	0.00	10.00	1.00	9260	3	241.00	0.12	−26.00	0.33	33.38	2.94
16	16.63	10.00	0.38	18,560	3	314.85	0.36	−29.00	8.45	26.32	6.46
17	24.63	4.89	0.01	13,460	4	299.70	0.41	−27.20	15.66	38.10	6.37
18	18.38	2.60	0.23	8900	3	294.80	0.25	−25.25	10.62	32.16	2.84
19	13.50	4.80	0.00	20,000	2	407.15	0.71	−28.15	9.42	26.11	2.39
20	9.75	5.95	0.43	15,380	1	502.60	0.59	−29.20	6.13	26.03	2.28
21	1.00	9.80	0.07	9560	2	839.53	0.68	−40.93	1.11	28.20	1.48
22	25.00	10.00	1.00	20,000	4	262.95	0.29	−24.45	9.53	30.88	24.29
23	1.13	0.00	0.63	15,680	2	219.55	0.45	−14.20	1.17	44.10	1.15
24	9.75	0.50	0.61	10,400	4	196.85	0.14	−23.75	9.85	45.77	1.70
25	14.63	10.00	1.00	13,400	1	625.45	0.63	−24.35	7.65	28.48	10.92
26	25.00	0.00	0.00	20,000	3	152.90	0.22	−18.85	17.54	45.25	5.97
27	10.88	10.00	0.50	8000	4	837.65	0.70	−26.70	9.66	30.09	4.61
28	18.38	2.60	0.23	8900	3	319.20	0.31	−25.65	10.88	35.64	2.99
29	0.00	0.00	1.00	20,000	1	309.25	0.45	−7.50	0.11	49.10	1.52
30	25.00	9.25	0.68	15,200	2	454.00	0.49	−26.20	10.14	36.51	35.39
31	25.00	3.70	0.60	19,400	1	365.95	0.47	−26.70	10.79	36.45	12.68
32	24.63	4.89	0.01	13,460	4	316.60	0.44	−27.10	15.06	35.48	4.96
33	0.00	9.65	0.05	20,000	1	377.25	0.37	−36.50	0.17	31.93	1.44
34	13.41	5.50	0.80	20,000	2	319.90	0.47	−25.20	8.82	25.56	4.55
35	25.00	8.10	0.00	20,000	1	625.45	0.57	−25.80	11.63	34.33	46.09
36	0.00	3.50	0.35	19,400	3	261.00	0.35	−26.85	0.13	34.56	1.31
37	25.00	9.25	0.68	15,200	2	632.00	0.67	−25.35	9.78	34.50	80.42
38	25.00	10.00	1.00	8000	3	1237.00	0.83	−23.40	10.64	28.34	35.35
39	13.38	0.00	0.05	12,860	1	164.10	0.20	−20.40	8.42	43.67	1.42

3. Results and discussion

3.1. Effect of the formulation and microfluidization conditions on the ADS, PdI and ζ of the HOPO emulsions

The droplet size is one of the most important factors affecting the dynamic stability of emulsions and is affected by the physicochemical properties of the emulsion components as well as the conditions of the processes involving the use of such emulsions. The droplet size was fitted to a model with an R^2 of 0.96 and a lack of fit less than 0.05 (see Table 2). This type of result allows the manipulation of the desired droplet size in an emulsion.

The concentrations of whey and HOPO as well as the pressure in the microfluidizer affected the droplet size response. The HOPO concentration ($p < 0.001$) was the variable that most affected the response, since a higher concentration resulted in a larger droplet size. As seen in Table 1, the minimum droplet size was 152.9 nm, while the maximum value was 1237 nm. Based on the above, the HOPO-pressure interaction was a highly significant interaction within the average droplet size behavior ($p = 0.0079$; see Table 2). Another important interaction was that of the whey-HOPO concentrations, which presented a direct relationship to the droplet size, and at higher concentrations of both compounds, the droplet size increased.

At higher concentrations of HOPO, greater number of droplets dispersed in the aqueous phase, and due to the proteins present in the whey, which form macromolecular layers which are covered with hydrophilic residues thus are highly soluble in water (Dissanayake, Ramchandran, Piyadasa, & Vasiljevic, 2013). Those layer are located around the droplets and thanks to thiol groups allows oleophilics interactions (disulphides bonds and thiol/disulphides interchange reactions (Nishanthi, Chandrapala, & Vasiljevic, 2018)), thus the structural stability in the emulsion increased, while the coalescence rate decreased (Floury, Desrumaux, & Lardières, 2000). This phenomenon is caused by the collision of oil droplets that generate a new droplet with a larger size than the initial droplet (Goibier, Lecomte, Leal-Calderon, & Faure, 2017). Thereby, to encapsulate in stable emulsion with higher concentration of HOPO is necessary greater whey concentration.

The pressure exerted by the microfluidizer also significantly affected the droplet size. As seen in Table 1, at a maximum pressure of 20,000 psi and considering the presence of all the compounds, the smallest droplet size was 500 nm. Likewise, higher cycle numbers in the microfluidizer showed how size was related to the variables. For a constant whey-HOPO ratio (see Fig. 1), the size decreased from approximately 600 nm (one cycle) to 200 nm (four cycles). A similar behavior was seen for the pressure-oil ratio, where, for constant values of pressure and HOPO concentration, the droplet size decreased as the number of microfluidization cycles increased. In the process of high-energy homogenization, the pressure exerted by the microfluidizer generates very intense disruptive forces capable of breaking the oil phase of the aqueous phase, resulting in the formation of very fine droplets of oil with more homogeneous sizes and which will subsequently be more evenly dispersed in the aqueous phase (Bai &

Table 2
ANOVA for the adjusted variables to response optimization design: ADS, PdI, ζ, conductivity, ST, and viscosity for nanoemulsions of HOPO.

	ADS, nm			PdI			ζ, mV			Conductivity, mS			ST (mN/m)			Viscosity, mPa·s		
	SS	df	*p*-Value	SS	df	*p*-Value	SS	df	*p*-Value	SS	df	*p*-Value	SS	df	*p*-Value	SS	df	*p*-Value
Model	$1.980 \cdot 10^{6}$	29	0.0017	1.19	29	0.0269	2109.64	29	< 0.0001	1114.17	29	< 0.0001	2399.75	29	0.0012	48.09	29	0.0003
A	96232.57	1	0.0101	0.094	1	0.0198	31.51	1	0.0296	562.29	1	< 0.0001	25.03	1	0.1503	28.30	1	< 0.0001
B	$5.338\ 10^{5}$	1	< 0.0001	0.23	1	0.0016	430.77	1	< 0.0001	12.07	1	< 0.0001	1227.11	1	< 0.0001	4.46	1	0.0003
C	4.55	1	0.9827	$4.109 \cdot 10^{-3}$	1	0.5686	238.98	1	< 0.0001	5.15	1	0.0002	0.093	1	0.9258	1.51	1	0.0097
D	$2.549 \cdot 10^{5}$	1	0.0005	0.012	1	0.3424	9.08	1	0.1990	0.22	1	0.2573	0.35	1	0.8576	0.062	1	0.5246
E	76690.82	3	0.1015	0.16	3	0.0313	0.076	3	0.9994	24.15	3	< 0.0001	59.37	3	0.1914	0.54	3	0.3416
AB			0.0022			0.0175			0.0054			0.0014			0.8921			0.0952
AC			0.1638			0.8381			0.0008			0.0237			0.7438			0.7033
AD			0.1263			0.0908			0.6512			0.0434			0.2927			0.2544
AE			0.0206			0.4573			0.3075			0.0112			0.2106			0.1946
BC			0.3328			0.6233			0.6497			0.1714			0.8740			0.6557
BD			0.0079			0.0206			0.4896			0.0011			0.6405			0.9648
BE			0.0942			0.2008			0.0518			0.0162			0.8639			0.9931
CD			0.1389			0.0729			0.0077			0.0318			0.9851			0.1887
CE			0.1411			0.2404			0.7083			0.0360			0.4174			0.8838
DE			0.0533			0.4048			0.4920			0.0021			0.5136			0.5560
A^2			0.5860			0.1108			0.6285			< 0.0001			0.0106			0.0124
B^2			0.1610			0.1917			0.0054			0.1086			0.0009			0.6385
C^2			0.6812			0.7366			0.3021			0.0906			0.2036			0.7852
D^2			0.0828			0.6779			0.3195			0.0140			0.6969			0.8983
Lack of Fit	65914.73	4	0.0538	0.080	4	0.0850	12.50	4	0.7265	1.04	4	0.0669	68.25	4	0.0906	0.90	4	0.1271
Pure Error	16498.89	5		0.026	5		30.00	5		0.29	5		22.87	5		0.37	5	
R^2	0.96			0.92			0.98			0.99			0.96			0.97		
R^2 – Adjusted	0.83			0.65			0.92			0.99			0.84			0.89		

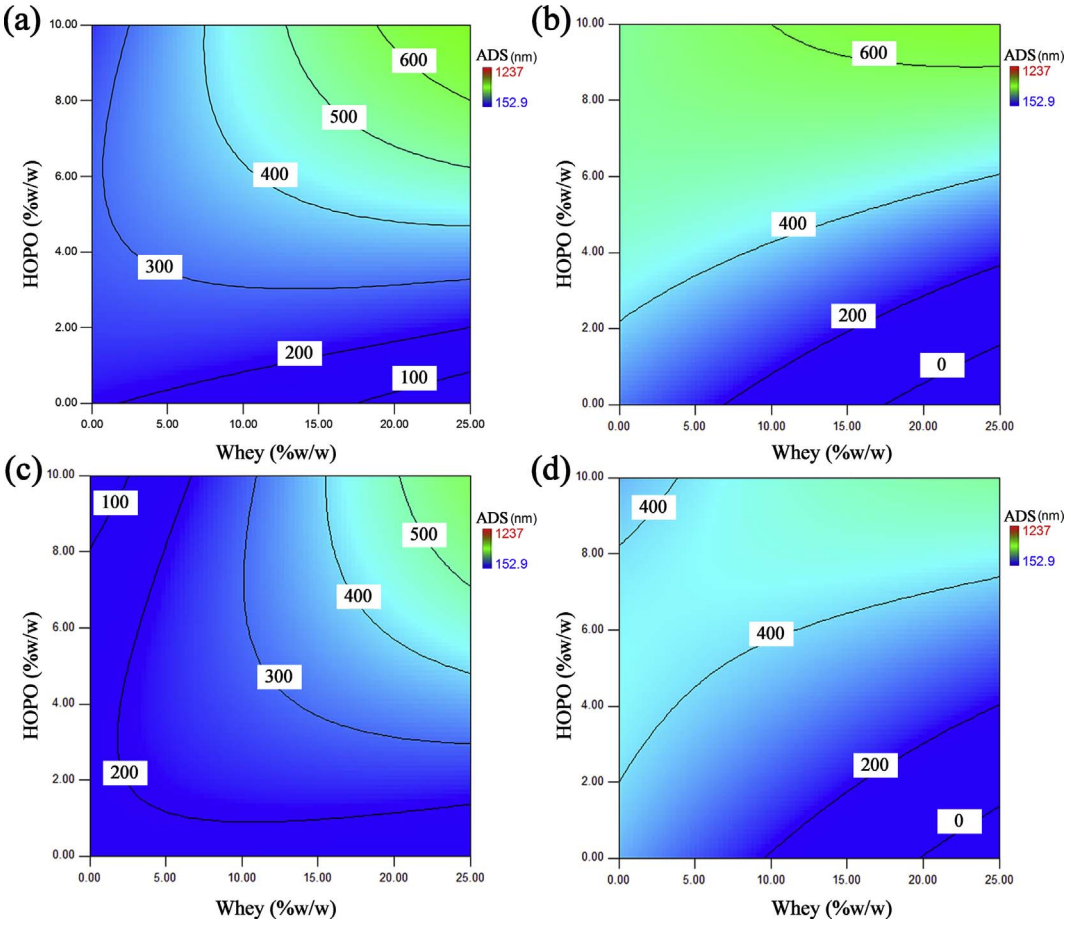

Fig. 1. Isoplots for adjusted variable ADS to the response design: (a) 1 cycle, (b) 2 cycles, (c) 3 cycles, and (d) 4 cycles of microfluidization.

McClements, 2016). On the other hand, at lower pressure, the droplet size increased (between 600 and 800 nm) due to the intrinsic conditions of the emulsions, especially the viscosity, which hinders the quality of the homogenization because it reduces the speed of the process and contributes to the recoalescence between droplets of oil (Lee & Norton, 2013).

Another variable associated with droplet size is the PdI, which is a dimensionless measurement of the droplet distribution throughout the phase, with values close to 0 indicating that the sample is monodispersed and values close to 1 indicating that the sample has a wide variety of sizes (Lancheros, Beleño, Godoy-Silva, & Guerrero, 2014). The ANOVA yielded a fit with an R^2 of 0.92. Table 2 shows that the model was significant with a p value less than 0.05 and a lack of fit of 0.85. As with size, the concentrations of whey and HOPO are the variables that most affected the PdI. In addition, the number of cycles is another variable that directly affects the behavior of the response (see Table 2). Because the pressure was not significant in the behavior of the PdI, the interaction of HOPO-pressure was significant in the model ($p = 0.0079$), as was the whey-HOPO ratio and whey-cycles ratio. It was seen that with a larger droplet size, the PdI was higher, varying between 0.12 and 0.83.

The droplet distribution was directly affected by the phenomena of recoalescence and protein aggregation, since these phenomena affect not only the droplet size but also the homogeneity of the distribution of the droplets in the aqueous phase, thus affecting the PdI measurement. On the other hand, although the number of cycles did not significantly affect the size, the number of cycles did significantly affect the PdI (Table 2). Floury et al. (2000) reported that increasing the number of cycles increases the energy supplied to the emulsion because, in addition to increasing the temperature, it promotes changes in the α and β bonds of the secondary structure and the rupture of the tertiary and quaternary structures of whey proteins, which in turn generates aggregation, specifically in β-lactoglobulin.

On the other hand, the ζ value is understood as the electro-kinetic potential difference between the dispersion medium and the slip plane (stationary layer of fluid attached to the dispersed particle) of moving particles, i.e., the difference in the electro-kinetic charge of the drop surface with respect to its dispersing medium (Liu, Shim, Wang, & Reaney, 2015). The ζ values of the nanoemulsions are shown in Table 1. The mathematical quadratic adjustment of the variable ζ in the ANOVA resulted in an R^2 of 0.98. Table 2 shows that the model was significant, with a p-value less than 0.05 and a lack of fit of 0.73, which suggests a high degree of model reliability in describing its behavior and the suitability of this model to predict the ζ values of nanoemulsions under similar conditions.

The Table 2 shows how the concentrations of whey, HOPO and gelatin significantly affected ($p < 0.05$) the behavior of ζ. Interactions between whey and HOPO (AB), whey and gelatin (AC), gelatin and pressure (CD) and HOPO concentration squared (B^2) affected the ζ of the nanoemulsion ($p < 0.05$) (see Table 2).

The droplets with ζ values more positive than +30 mV or more negative than −30 mV are usually considered stable, since the electrical charge of droplets is strong enough to assume that repulsive forces between droplets are predominant in the nanoemulsion system (Heurtault, Saulnier, Pech, Proust, & Benoit, 2003). A decrease in the ζ value could be attributed to an over-processing or over-energization of the system, resulting in the recoalescence of the new drops formed (Sadeghpour & Dabir, 2015). In this sense, absolute values less than or greater than 25 mV are indicative of flocculated and deflocculated emulsions, respectively.

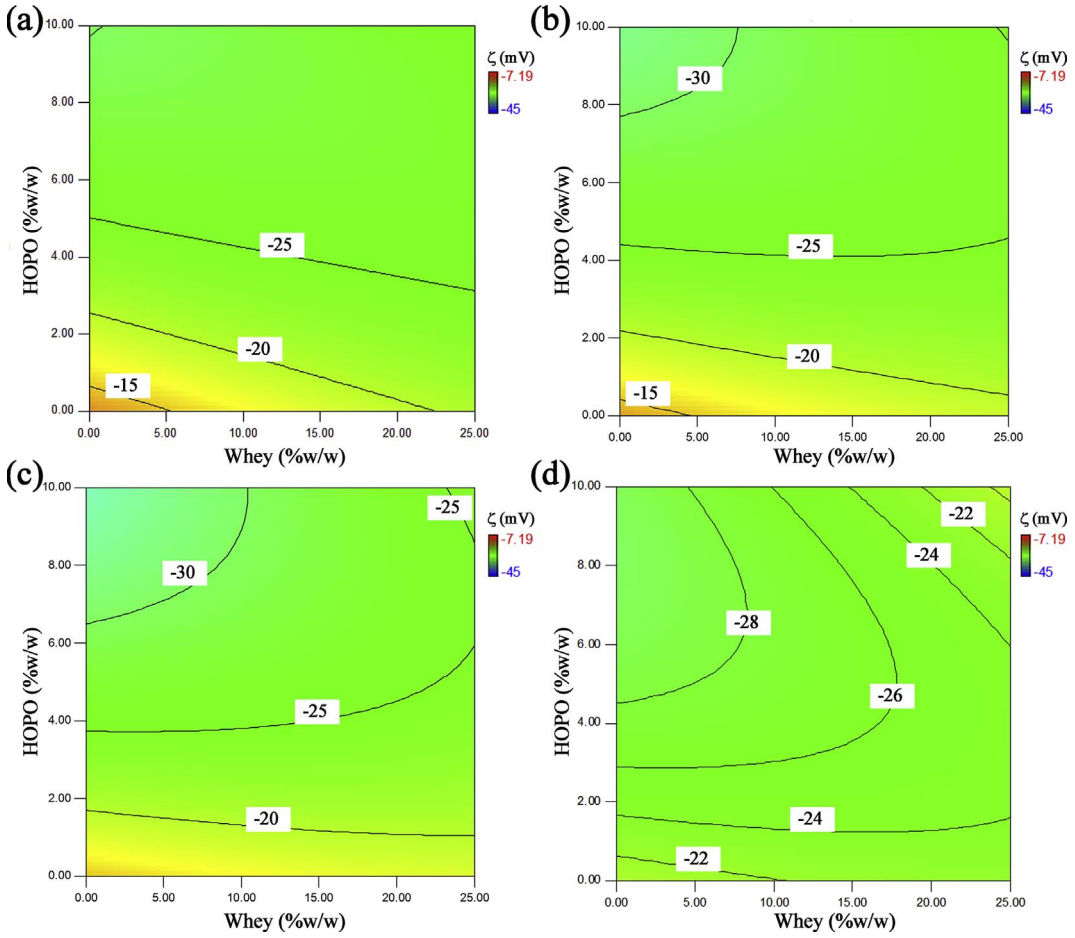

Fig. 2. Isoplots for adjusted variable ς to the response design: (a) 1 cycle, (b) 2 cycles, (c) 3 cycles, and (d) 4 cycles of microfluidization.

In general, the ζ values of nanoemulsions were more negative when the oil concentration increased, and the whey concentration decreased for all of the microfluidization cycles. Similar results were obtained by Ricaurte et al. (2016) when evaluating the most favorable conditions for the microfluidization, formulation and storage of HOPO nanoemulsions using whey powder to produce stable nanoemulsions. This effect can be observed in Fig. 2. In this figure, how the number of cycles affected ζ can be observed. In this manner, working with microfluidization cycles greater than 1 (see Fig. 2B, C, D) allows emulsions with more negative ζ values (more stable) to be obtained. Likewise, high concentrations of HOPO and intermediate concentrations of whey (10%, w/w) allow more negative values of ζ to be obtained. On the other hand, when working with one or two microfluidization cycles (Fig. 2A and 2B), when low whey and HOPO concentrations are used, less negative ζ values are obtained (less stable). This can be associated with a suitable droplet size that balances the charge of oil droplets by balancing the surface tension of the system.

It is important to highlight the relationship among ADS, ζ and stability. Thus, for molecules and droplets that are smaller, it will confer stability (higher values of ζ). Finally, the prediction equations of ADS, PdI and ζ for each one of the microfluidization cycles are listed in Supplement 1. These variables fit the response optimization design, with R^2 values of 0.96, 0.92, and 0.98, respectively. These high values of R^2 indicate the suitability of the model to correctly predict the values of these variables for any single nanoemulsion. Other authors have also obtained high R^2 values by adjusting the behaviors of these variables to a linear-type quadratic model in HOPO nanoemulsions (Ricaurte et al., 2016).

3.2. Surface tension

Surface tension (ST) is the phenomenon caused by the cohesion forces among individual liquid molecules that depend, among others, on the surrounding medium and the temperature (Kane & Sternheim, 2007). According to the ANOVA results, the ST variable was fitted to a quadratic model ($R^2 = 0.96$); this model was significant, with a p-value lower than 0.05 and a lack of fit greater than 0.05, suggesting that it can predict the value of ST for any nanoemulsion. The concentration of HOPO (B) and the quadratic factors of whey (A^2) and oil (B^2) concentrations affected ($p < 0.05$) the minimum (21.962 mN/m) and maximum (51.420 mN/m) values of ST (Table 2). Based on these results, we summarized in Supplement 1 the equations to predict ST from the model parameters for each studied cycle.

The concentration of HOPO influenced superficial tension; this may be due to the HOPO intrinsic tension, 30.8 mN/m, and the lecithin activity. Because of the lecithin constant concentration ratio with respect to the oil (10% w/w), it played as a surfactant in the emulsion, reducing the ST at the contact surface between the two phases. On the other hand, the content of solids may vary the ST since solids like proteins –beta-lactoglobulin and alpha-lactalbumin–, lipids, lactose, minerals, and vitamins reduce the thermodynamic contact among molecules and, depending on the component surface activity, they can increase or decrease tension. González-Tello, Camacho, Guadix, Luzón, and González (2009) found that tension decreased at whey concentrations lower or equal to 0.05% w/w, while it increased or remained constant at higher concentrations, up to 0.30% w/w. Whey is known as a high-surface-activity material, used to achieve maximum surface activities (Adhikari, Howes, Shrestha, & Bhandari, 2014), which may have favored the ST increase in the nanoemulsions.

3.3. Conductivity

Conductivity is the ability of a materia to conduct an electric current, and depends on the bonds present in the material, the atomic structure, and temperature (Portis & Young, 2006).

Based on the ANOVA results, the conductivity response variable fitted to a quadratic model ($R^2 = 0.99$), with a p-value lower than 0.05 and a lack-of-fit greater than 0.05 (Table 2), indicating that the model is suitable to predict the conductivity value for any nanoemulsion. The concentrations of whey, oil, and gelatin, the number of cycles, and some of the interactions (see Table 2) influenced significantly over the conductivity ($p < 0.05$). Furthermore, the equations for the prediction of conductivity from the model parameters of the model for each of the cycles are shown in Supplement 1.

In general, the presence of whey influenced the conductivity, with the lowest value (0.111 mS) observed when whey was absent, and the highest (17.54 mS) when whey was present. On the other hand, the presence of HOPO resulted in intermediate and low values, which was expected since the conductivity of HOPO (0.15–0.17 mS) is similar to the lower values obtained (Rincón & Martínez, 2009), which are even lower than those of water. This finding agrees with McClements (2004), who stated that the conductivity of an emulsion increases when the water content is greater than the oil content.

The effect of the whey in increasing the conductivities of the nanoemulsions might be due to the solid content. Callejas Hernández, Prieto, Cruz, Santillán, and Marzo (2012) showed that total solids –mainly dissolved solids– had the greatest contribution to conductivity. Additionally, Zhuang, Zhou, Nguyen, and Hourigan (1997) demonstrated that, mainly, H^+ and Cl^- ions determined whey conductivity, whereas proteins and fat did not conduct and impeded the mobility of ions. Although whey has conductivities greater than 8 mS/cm, they can vary according to its acidity.

3.4. Flow curves

The results obtained from the ANOVA for the viscosity response variable are shown in Table 2. The results were fitted to a quadratic type model with an R^2 of 0.97. The table indicates that the model was significant, with a p-value less than 0.05 and a lack of fit greater than 0.05, which indicates the suitability of the model to predict the viscosity value for any one nanoemulsion.

The viscosity at a shear rate of 75 s^{-1} varied within the range of values between 1.15 and 80.42 mPa·s (see Table 1). The highest viscosity was obtained for a nanoemulsion with high contents of whey, HOPO and gelatin.

The results (see Table 2) showed that the concentrations of whey, HOPO and gelatin and whey concentration squared (A^2) significantly affected the viscosity of the emulsion ($p < 0.05$). An increasing the whey concentration, oil and gelatin increased the viscosity of the emulsion.

The principal role of thickening agents in food emulsions is to increase the viscosity of the aqueous phase of O/W emulsions. This is because a higher viscosity was observed with a higher solid concentration (whey, oil and gelatin) in the nanoemulsion.

In the food industry, the most commonly used thickening agents are usually polysaccharides or proteins in O/W emulsions (McClements, 2004). In this sense, Li, Ma, and Cui (2014) studied curcumin nanoemulsions stabilized by isolated whey proteins and observed that the viscosity increased at higher protein concentrations.

On the other hand, droplet aggregation often leads to a large increase in the emulsion viscosity (McClements, 2004), which can explain the larger droplet size found in more viscous nanoemulsions. It has been observed that the higher the viscosity of the oil phase is, the higher the emulsion droplet size (Qian & McClements, 2011). In fact, as the oil viscosity increases, the disruptive forces needed to deform the oil droplets during homogenization are higher (Håkansson, Trägårdh, & Bergenståhl, 2009). Namely, (Wooster et al., 2008) observed droplet sizes of approximately 120 nm in nanoemulsions formulated with high-viscosity oils, whereas nanoemulsions containing low viscosity oils presented droplet sizes of approximately 80 nm. Likewise, the aggregation of droplets contributes to decreased emulsion stability, which would explain the larger ζ values (less negative) obtained in the more viscous nanoemulsions (McClements & Rao, 2011).

The microfluidization pressure employed and the number of microfluidization cycles did not have statistically significant effects ($p > 0.05$) on the viscosity of the emulsion obtained. Different results were obtained by Salvia-Trujillo, Qian, Martín-Belloso, and McClements (2013). They observed that microfluidization treatment had a significant effect on the viscosities of nanoemulsions, since it significantly decreased with increasing the treatment pressure and the number of cycles.

Likewise, none of the interactions between the different factors studied (see Table 2) were significant ($p > 0.05$). The equations for the prediction of the viscosity from the model parameters for each of the cycles studied are shown in Supplement 1.

3.5. HOPO nanoemulsion stability

According to the optimization performed using the criterion of desirability, two emulsions were obtained, one with a minimum droplet size (min-opt) and one with a maximum droplet size (max-opt), both with the ζ values furthest from zero, that is, more stable. The formulation and process conditions as well as predicted values of both droplet size and ζ are shown in Table 3.

3.5.1. Thermal stability of nanoemulsions

The thermograms showing the thermal and mass behaviors of HOPO nanoemulsions with minimum and maximum droplet sizes and they are shown in Fig. 3a and 3b. The percentage of weight loss was lower for the emulsion with a larger droplet size, with a maximum mass loss of 79%, compared to the smaller droplet size with 44% maximum mass loss. This is due to the lower availability of water with respect to the surface area that the oil occupies.

Different matrices containing palm oil showed that the loss of weight in the thermogram is because the emulsion with the minimum size contains less oil, and the higher weight loss may be associated with this. The formulation has a significant effect on the stability of the nanoemulsion, since in the case of the min-opt, the highest content is water, in contrast to the max-opt, whose percentage of water is displaced by the HOPO content.

Table 3
Experimental optimum conditions obtained by for the response optimization design for ADS and ζ: experimental values versus values of prediction equations and Ostwald ripening rate.

Run	Whey concentration (%w/w)	HOPO concentration (%w/w)	Gelatin concentration (%w/w)	Pressure (psi)	Cycles	Desirability	ADS (nm)		ζ (mV)		Ostwald ripening rate ω × 10^{-23}, m^3/s	Regression coefficient R^2
							Experimental	Model	Experimental	Model		
Min-opt	10	5	0.01	20,000	3	0.887	340.2	306.3	−33.2	−31.3	5	0.97
Max-opt	20	10	0.01	8000	2	0.828	1153.0	1054.0	−36.2	−33.0	8	0.98

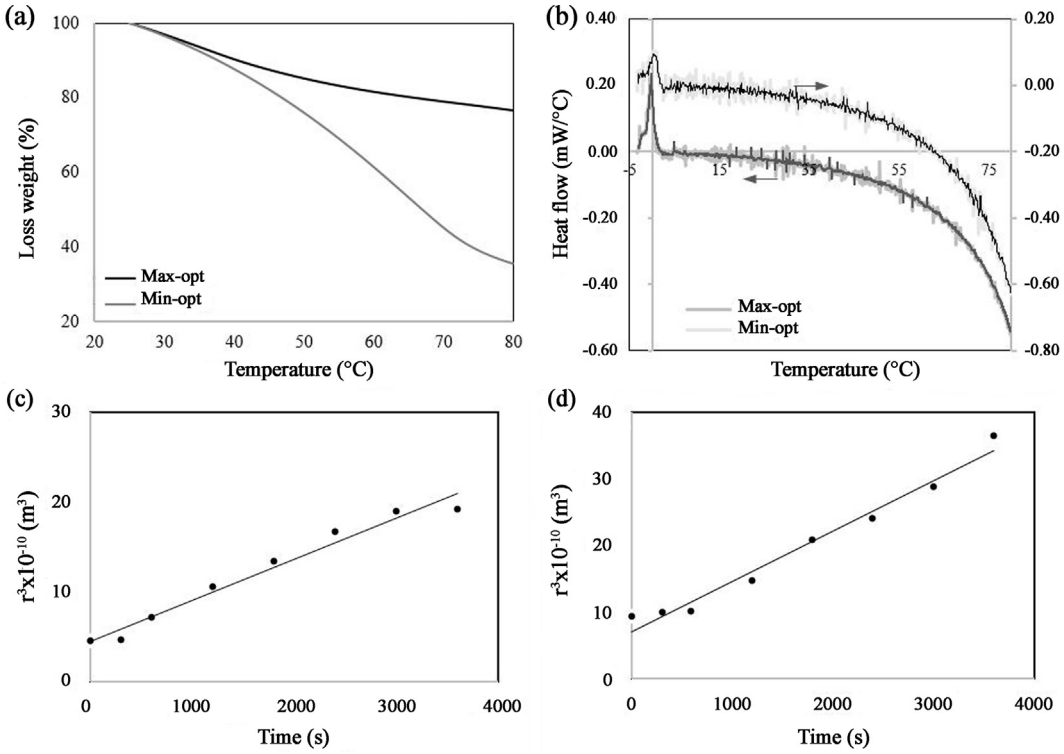

Fig. 3. HOPO nanoemulsion stability: (a) thermogram of loss weight, (b) thermogram of heat flow both in function of the temperature and the cube of the droplet radius (r^3) as a function of time for (c) minimum and (d) maximum ADS.

On the other hand, DSC is one of the most widely used thermal characterization techniques, since it provides information on the heat exchange between the sample and a reference as a function of time or temperature (Dalmazzone1, Noïk, & Clausse, 2009). DSC thermograms for optimized HOPO emulsions showed good thermal stabilities, as they exhibited small changes in heat flow, which were associated with the loss of water from the system and the low heat transfer of the system. In addition, as has been reported, the larger the droplets that compose the emulsion are, the greater the instability and the higher the freezing temperature of the water (see Fig. 3b) (Clausse, 1998).

Finally, Fig. 3b shows the formation of a peak between approximately −5 and 5 °C, which is associated with the solidification of the emulsion (specifically, the dispersant phase) corresponding to an exothermic signal (Clausse, 1998). However, it is not attributed to any particular behavior. In DSC analyses performed on whey (data not shown), the peak denaturation of proteins was initiated at 90 °C and reached its maximum value at 131 °C. Therefore, the emulsions allowed a more thermally stable colloidal system to be formed due to the affinity between the hydrophobic areas of the whey proteins and the HOPO, thus reinforcing the interface.

3.5.2. Destabilization mechanism of HOPO nanoemulsions

The destabilization mechanism of the emulsions is very important to improve the formation and stability of systems with such matrices (Agboola, Singh, Munro, Dalgleish, & Singh, 1998). Understanding the behavior of this process and establishing parameters that allow comparison between emulsions to determine their stability would allow their more appropriate use. Therefore, in this work, the establishment of the Ostwald ripening coefficient was proposed. This destabilization phenomenon implies that the droplets of the dispersed phase change from smaller sizes to larger ones (Schmitt, Arditty, & Leal-Calderon, 2004).

Nanoemulsions are defined as stable when a small droplet size has a high coefficient of Ostwald ripening (Noor El-Din et al., 2013). Fig. 3c and 3d show the relationship between the cube of the droplet radius (r^3) and time (t). This relationship allowed the value of the coefficient of Ostwald ripening to be calculated using the slope of the line, as shown in Table 3.

The correlation coefficient (R^2) between the cube of the droplet radius and time presented a good fit for both emulsions, min-opt and max-opt, with values of 0.97 and 0.98, respectively. This result indicates that the forces that drive the destabilization of HOPO nanoemulsions respond to an Ostwald ripening mechanism.

The speed associated with destabilization was higher for nanoemulsions with the minimum droplet size (see Table 3) because, as has been reported, these emulsions are more unstable in thermodynamic terms due to Brownian motion associated with smaller droplets is greater than for larger ones, as reported by Joye, Davidov-Pardo, and McClements (2014).

The droplet size for the min-opt increases up to 1.6 times with respect to the initial radius value, while for the max-opt, this value is 0.6 times the initial radius value during the evaluation period for destabilization. Finally, it was possible to establish that the rate of Ostwald ripening is high, that is to say, it describes the destabilization mechanism of highly stable HOPO emulsions since the values of this rate are higher in comparison to those reported by Noor El-Din et al., (2013) for O/W type emulsions. This high stability can be attributed to both the microfluidization conditions and the emulsifiers employed, since gelatin is slightly active on the surface and acts as an emulsifier. Stable O/W emulsions have even been obtained with gelatin concentrations equal or greater than 4 wt% (Bouyer, Mekhloufi, Rosilio, Grossiord, & Agnely, 2012). Lecithin is an emulsifier widely used in the food industry because it is non-allergic and bio-friendly. The use of both emulsifiers consisting of macromolecules constructed a route of inhibition for the destabilization by Ostwald ripening (Donsì & Ferrari, 2016). Therefore, by obtaining stable HOPO emulsions, additional processes such as cooling (used to improve the half-life and stability of the emulsion (Ricaurte et al., 2016)) are not required for their storage and subsequent use.

4. Conclusions

HOPO nanoemulsions obtained by microfluidization showed good chemical interactions and therefore good physical properties (droplet size, zeta potential, conductivity and viscosity), which allows their use and incorporation in different food matrices. Furthermore, the thermal and thermodynamic stabilities of HOPO emulsions were high due to the use of food-grade emulsifiers such as lecithin and gelatin. It was possible to establish the rate of Ostwald ripening as a parameter to determine both the mechanism of destabilization as well as the degree of stability of the HOPO emulsions. In short, the droplet size of the emulsion remains a determining factor when formulating physically and thermally stable emulsions. Finally, the response surface methodology employed showed good fit and predictive behavior models of the different response variables, which makes them highly reliable and facilitates the prediction of desirable emulsion characteristics for the food industry.

Acknowledgment

The authors thank the Universidad de La Sabana for its help in this investigation through the funding of the ING-170-2016 project. Furthermore, we thanks to Cenipalma, Colombia for kindly supplying the High Oleic Palm Oil used in this study and to Alexandra Mondragón Serna, Leader of the project of Health and Nutrition of Cenipalma. Additionally, we thanks to Banco de Desarrollo de América Latina (CAF) for the support to this research. Leidy Ricaurte acknowledges COLCIENCIAS for the doctoral scholarship (grant number 727-2015).

Appendix A. Supplementary data

Supplementary data associated with this article can be found, in the online version, at http://dx.doi.org/10.1016/j.foodchem.2018.02.102.

References

Adhikari, B., Howes, T., Shrestha, A., & Bhandari, B. R. (2014). Erratum: Effect of surface tension and viscosity on the surface stickiness of carbohydrate and protein solutions (Journal of Food Engineering (2007) 79 (1136–1143)). *Journal of Food Engineering, 129*, 53. http://dx.doi.org/10.1016/j.jfoodeng.2013.12.028.

Agboola, S. O., Singh, H., Munro, P.a., Dalgleish, D. G., & Singh, A. M. (1998). Destabilization of oil-in-water emulsions formed using highly hydrolyzed whey proteins. *Journal of Agricultural and Food Chemistry, 46*(1), 84–90. http://dx.doi.org/10.1021/jf970365b.

Bai, L., & McClements, D. J. (2016). Development of microfluidization methods for efficient production of concentrated nanoemulsions: Comparison of single- and dual-channel microfluidizers. *Journal of Colloid and Interface Science, 466*, 206–212. http://dx.doi.org/10.1016/j.jcis.2015.12.039.

Bouyer, E., Mekhloufi, G., Rosilio, V., Grossiord, J.-L., & Agnely, F. (2012). Proteins, polysaccharides, and their complexes used as stabilizers for emulsions: Alternatives to synthetic surfactants in the pharmaceutical field? *International Journal of Pharmaceutics, 436*(1–2), 359–378. http://dx.doi.org/10.1016/j.ijpharm.2012.06.052.

Callejas Hernández, J., Prieto, G., Cruz, R., Santillán, M., & Marzo, M. (2012). Caracterización fisicoquímica de un lactosuero: Potencialidad de recuperación de fósforo. *Acta Universitaria, 22*(1), 11–18.

Clausse, D. (1998). Thermal behaviour of emulsions studied by differential scanning calorimetry. *Journal of Thermal Analysis and Calorimetry, 51*(1), 191–201. http://dx.doi.org/10.1007/BF02719021.

Cuellar, M. (2016). Experiencias en la producción y mercadeo del aceite de palma alto oleico. *Revista Palmas, 37*, 322–330.

Dalmazzone1, C., Noïk, C., & Clausse, D. (2009). Application of DSC for emulsified system characterization. Oil & Gas Science and Technology-Revue ..., 64(1), 543–555. https://doi.org/DOI: 10.2516/ogst:2008041.

Dissanayake, M., Ramchandran, L., Piyadasa, C., & Vasiljevic, T. (2013). Influence of heat and pH on structure and conformation of whey proteins. *International Dairy Journal, 28*(2), 56–61. http://dx.doi.org/10.1016/j.idairyj.2012.08.014.

Donsì, F., & Ferrari, G. (2016). Essential oil nanoemulsions as antimicrobial agents in food. *Journal of Biotechnology, 233*, 106–120. http://dx.doi.org/10.1016/j.jbiotec.2016.07.005.

Floury, J., Desrumaux, A., & Lardières, J. (2000). Effect of high-pressure homogenization on droplet size distributions and rheological properties of model oil-in-water emulsions. *Innovative Food Science & Emerging Technologies, 1*(2), 127–134. http://dx.doi.org/10.1016/S1466-8564(00)00012-6.

Goibier, L., Lecomte, S., Leal-Calderon, F., & Faure, C. (2017). The effect of surfactant crystallization on partial coalescence in O/W emulsions. *Journal of Colloid and Interface Science, 500*, 304–314. http://dx.doi.org/10.1016/j.jcis.2017.04.021.

González-Tello, P., Camacho, F., Guadix, E. M., Luzón, G., & González, P. A. (2009). Density, viscosity and surface tension of whey protein concentrate solutions. *Journal of Food Process Engineering, 32*(2), 235–247. http://dx.doi.org/10.1111/j.1745-4530.2007.00213.x.

Håkansson, A., Trägårdh, C., & Bergenståhl, B. (2009). Studying the effects of adsorption, recoalescence and fragmentation in a high pressure homogenizer using a dynamic simulation model. *Food Hydrocolloids, 23*(4), 1177–1183. http://dx.doi.org/10.1016/j.foodhyd.2008.10.003.

Heurtault, B., Saulnier, P., Pech, B., Proust, J.-E., & Benoit, J.-P. (2003). Physico-chemical stability of colloidal lipid particles. *Biomaterials, 24*(23), 4283–4300.

Jeong, I.-J., & Kim, K.-J. (2009). An interactive desirability function method to multi-response optimization. *European Journal of Operational Research, 195*(2), 412–426. http://dx.doi.org/10.1016/j.ejor.2008.02.018.

Joye, I. J., Davidov-Pardo, G., & McClements, D. J. (2014). Nanotechnology for increased micronutrient bioavailability. *Trends in Food Science & Technology, 40*(2), 168–182. http://dx.doi.org/10.1016/j.tifs.2014.08.006.

Kane, J. W., & Sternheim, M. M. (2007). *Physics.* Massachusetts: Reverté.

Hacienda La Cabaña. (2012). Aceite crudo de palma alto oleico-Ficha técnica de calidad.

Lancheros, R. J., Beleño, J.Á., Godoy-Silva, R. D., & Guerrero, C. A. (2014). Producción de nanopartículas de PLGA por el método de emulsión y evaporación para encapsular N-Acetilcisteína (NAC). *Journal of the Faculty of Science, 92*, 161–168.

Lee, L., & Norton, I. T. (2013). Comparing droplet breakup for a high-pressure valve homogeniser and a Microfluidizer for the potential production of food-grade nanoemulsions. *Journal of Food Engineering, 114*(2), 158–163. http://dx.doi.org/10.1016/j.jfoodeng.2012.08.009.

Li, M., Ma, Y., & Cui, J. (2014). Whey-protein-stabilized nanoemulsions as a potential delivery system for water-insoluble curcumin. *LWT – Food Science and Technology, 59*(1), 49–58. http://dx.doi.org/10.1016/j.lwt.2014.04.054.

Liu, J., Shim, Y. Y., Wang, Y., & Reaney, M. J. T. (2015). Intermolecular interaction and complex coacervation between bovine serum albumin and gum from whole flaxseed (Linum usitatissimum L.). *Food Hydrocolloids, 49*, 95–103. http://dx.doi.org/10.1016/j.foodhyd.2015.02.035.

McClements, D. J., & Rao, J. (2011). Food-grade nanoemulsions: Formulation, fabrication, properties, performance, biological fate, and potential toxicity. *Critical Reviews in Food Science and Nutrition, 51*(4), 285–330. http://dx.doi.org/10.1080/10408398.2011.559558.

McClements, D. J. (2004). Food Emulsion Principle,Practices, and Techniques.

Nirmala, R., Park, H. M., Navamathavan, R., Kang, H. S., El-Newehy, M. H., & Kim, H. Y. (2011). Lecithin blended polyamide-6 high aspect ratio nanofiber scaffolds via electrospinning for human osteoblast cell culture. *Materials Science and Engineering C, 31*(2), 486–493. http://dx.doi.org/10.1016/j.msec.2010.11.013.

Nishanthi, M., Chandrapala, J., & Vasiljevic, T. (2018). Physical properties of selected spray dried whey protein concentrate powders during storage. *Journal of Food Engineering, 219*, 111–120. http://dx.doi.org/10.1016/j.jfoodeng.2017.09.021.

Noor El-Din, M. R., El-Hamouly, S. H., Mohamed, H. M., Mishrif, M. R., & Ragab, A. M. (2013). Water-in-diesel fuel nanoemulsions: Preparation, stability and physical properties. *Egyptian Journal of Petroleum, 22*(4), 517–530. http://dx.doi.org/10.1016/j.ejpe.2013.11.006.

Obahiagbon, F. I. (2012). A review: Aspects of the African Oil Palm (Elaeis guineesis jacq.) and the implications of its bioactives in human health. *American Journal of Biochemistry and Molecular Biology, 2*, 106–119.

Portis, A. M., & Young, H. D. (2006). *Electrónica de semiconductores.* Nueva York: Reverté.

Primozic, M., Duchek, A., Nickerson, M., & Ghosh, S. (2017). Effect of lentil proteins isolate concentration on the formation, stability and rheological behavior of oil-in-water nanoemulsions. *Food Chemistry, 237*, 65–74. http://dx.doi.org/10.1016/j.foodchem.2017.05.079.

Qian, C., & McClements, D. J. (2011). Formation of nanoemulsions stabilized by model food-grade emulsifiers using high-pressure homogenization: Factors affecting particle size. *Food Hydrocolloids, 25*(5), 1000–1008. http://dx.doi.org/10.1016/j.foodhyd.2010.09.017.

Ricaurte, L., de Perea-Flores, M. de J., Martinez, A., & Quintanilla-Carvajal, M. X. (2016). Production of high-oleic palm oil nanoemulsions by high-shear homogenization (microfluidization). *Innovative Food Science & Emerging Technologies, 35*, 75–85. http://dx.doi.org/10.1016/j.ifset.2016.04.004.

Rincón, M. S. M., & Martínez, C. D. M. (2009). Análisis de las propiedades del aceite de palma en el desarrollo de su industria. *Revista Palmas, 30*(2), 11–24.

Sadeghpour, S. G., & Dabir, B. (2015). Three-factor response surface optimization of nano-emulsion formation using a microfluidizer. *Journal of Food Science and Technology, 52*(5), 2558–2571. http://dx.doi.org/10.1007/s13197-014-1363-1.

Salvia-Trujillo, L., Qian, C., Martín-Belloso, O., & McClements, D. J. (2013). Influence of particle size on lipid digestion and β-carotene bioaccessibility in emulsions and nanoemulsions. *Food Chemistry, 141*(2), 1472–1480. http://dx.doi.org/10.1016/j.foodchem.2013.03.050.

Schmitt, V., Arditty, S., & Leal-Calderon, F. (2004). Stability of concentrated emulsions. *Emulsions: Structure, stability and interactions* (pp. 607–620). (2nd ed.). New York: Springer-Verlag. http://dx.doi.org/10.1007/978-0-387-39683-5.

Segall, S. D., & Artz, W. E. (2005). Frying lipids. *Handbook of functional lipids* (pp. 185–187). CRC Press.

Teixeira, M. C., Severino, P., Andreani, T., Boonme, P., Santini, A., Silva, A. M., & Souto, E. B. (2017). d-α-tocopherol nanoemulsions: Size properties, rheological behavior, surface tension, osmolarity and cytotoxicity. *Saudi Pharmaceutical Journal, 25*(2), 231–235. http://dx.doi.org/10.1016/j.jsps.2016.06.004.

Wooster, T. J., Golding, M., & Sanguansri, P. (2008). Impact of oil type on nanoemulsion formation and ostwald ripening stability. *Langmuir, 24*(22), 12758–12765. http://dx.doi.org/10.1021/la801685v.

Zhuang, Y., Zhou, W., Nguyen, M. H., & Hourigan, J. A. (1997). Determination of protein content of whey powder using electrical conductivity measurement feasible for many smaller companies. *International Dairy Journal, 7*(10), 647–653.